Cell Death & Differentiation

ARTICLE

Conditional deletion of platelet derived growth factor receptor alpha (Pdgfra) in urorectal mesenchyme causes mesenchyme apoptosis and urorectal developmental anomalies in mice

Chen Qian[1,2] · Zhongluan Wu[1] · Roy Chun-Laam Ng[1,3] · Maria-Mercè Garcia-Barceló[1,4] · Zheng-Wei Yuan[5] · Kenneth Kak Yuen Wong[1] · Paul Kwong Hang Tam[1,4] · Vincent Chi Hang Lui[1,4]

Abstract

In mammals, urorectal development starts at early embryonic stage, defective urorectal development results in anorectal malformations, which are common congenital developmental defects of the anus and the urethra in newborns. The etiology and embryology of the defects are still largely unknown. Platelet-derived growth factor receptor alpha (Pdgfra) is a cell surface receptor tyrosine kinase, upon binding to its ligands (Pdgfa-d), mediates intracellular signaling and regulates embryonic development. The expression of Pdgfra is tightly regulated in the developing urorectal mesenchyme, and its dysregulation is associated with urorectal defects in animals with urorectal defects. Knockout of *Pdgfra* induces early embryo lethality which precludes investigation of *Pdgfra* in urorectal development. To address the temporal requirement of *Pdgfra* in urorectal development, we conditionally deleted *Pdgfra* in *Pdgfra*-expressing tissues using a tamoxifen inducible *Cre-loxP* approach in mice, examined the urorectal development in *Pdgfra* conditional knockout (*Pdgfra-cKO*) embryos. We showed that conditional deletion of *Pdgfra* in *Pdgfra*-expressing tissues at E10-E11 caused cloaca septation defect, anteriorly displaced anus, defective urogenital folds development and abnormal urethra tubularization in both male and female mice. Furthermore, we showed that *Pdgfra* was required for the survival of urorectal mesenchyme, deletion of *Pdgfra* caused apoptosis in the peri-cloacal, the peri-urethra and the urorectal septum mesenchyme of *Pdgfra-cKO* mutants, associated with an induction of p53, Ndrg1 and activation of caspase-3 in *Pdgfra-cKO* embryos. In conclusion, Pdgfra is required for the development and survival of the urorectal mesenchyme in embryo, dysregulated Pdgfra signaling induced urorectal defects in mice resembling human congenital diseases of anorectal malformations and hypospadias. Perturbation of PDGFRA signaling may contribute to anorectal malformations and hypospadias in human.

Introduction

The external genitalia development could be divided into three phases: genital tubercle (GT) outgrowth, cloaca septation and urethra tubularization. GT outgrowth is initiated by peri-cloaca mesenchymal proliferation resulting in a paired genital swelling on either side of the cloaca (an endoderm-lined cavity at the caudal end of mammalian embryos), that fuse medially accompanied by the formation

This author contributed equally: Chen Qian.

Edited by M. Piacentini

Electronic supplementary material The online version of this article (https://doi.org/10.1038/s41418-018-0216-2) contains supplementary material, which is available to authorized users.

✉ Vincent Chi Hang Lui
vchlui@hku.hk

1 Department of Surgery, LKS Faculty of Medicine, The University of Hong Kong, Hong Kong, SAR, China

2 Department of Obstetrics and Gynecology, Renji Hospital Affiliated to Shanghai Jiaotong University School of Medicine, Shanghai, China

3 Department of Medicine, LKS Faculty of Medicine, The University of Hong Kong, Hong Kong, SAR, China

4 Dr Li Dak-Sum Research Centre, The University of Hong Kong-Karolinska Institutet Collaboration in Regenerative Medicine, Hong Kong, China

5 Key Laboratory of Health Ministry for Congenital Malformation, Shengjing Hospital, China Medical University, Shenyang, China

of the urethral plate epithelium (the future urethra epithelium) at the ventral midline of the GT to form the future external genitalia [1]. During cloaca septation, the urorectal septum (urs), an endoderm-lined mesenchyme, proliferates and elongates from the ventral body wall to the cloaca membrane (cm). The proximal cm starts to regress when the apical urs endoderm approaches the cm leading to the urethral duct and the anal opening formation, marking the completion of cloaca septation. The external genitalia development prior to the urethra tubularization is androgen-independent and is morphologically indistinguishable between male and female embryos [2]. In contrast, the urethra tubularization phase is androgen-dependent and hence different between males and females in humans and many other animal species.

In male, the external genitalia develop into the penis with the urethral tube running along its whole length. Whereas in female, the external genitalia develop into the clitoris, the urethra is shorter and emerges above the vaginal opening. Incomplete urethra tubularization results in hypospadias in male, which involves an abnormally placed urethra orifice at the ventral side of the penis. The corresponding defect in females is an opening of the urethra into the vagina. Hypospadias are among the most common birth defects of the male genitalia, and the worldwide incidence ranges from 5 to 34 per 10,000 live births [3]. In most cases, the cause of this birth defect is still obscure. Hence, a better understanding of the developmental mechanisms of genital tubercle will provide insights on the pathogenesis of hypospadias.

Platelet-derived growth factor (PDGF) was characterized as a serum protein that stimulated the growth and migration of vascular smooth muscle cells, fibroblasts and glial cells [4, 5, 6]. In human and mouse, the PDGF family is composed of four different polypeptide chains (PDGF-A, B, C, and D) encoded by four different genes (PDGF-A, B, C, and D) [7, 8, 9]. PDGFs are secreted as homodimeric proteins (PDGF-AA, BB, CC, and DD), and only PDGF-A and PDGF-B are able to form heterodimer of PDGF-AB [9]. The PDGF signaling network consists of four ligands, PDGFA-D, and two cell surface receptors, PDGFRA and PDGFRB [10, 11]. PDGF-PDGFR signaling controls cellular proliferation, survival, migration and differentiation [12, 13].

PDGFRA is a transmembrane receptor tyrosine kinase with an extracellular ligand binding domain and an intracellular tyrosine kinase domain, and binds homodimers of PDGF-A, PDGF-B, PDGF-C and heterodimer PDGF-AB [10, 11]. PDGF binding dimerizes PDGFRAs and activates the kinase activity, which in turn auto-phosphorylate intracellular tyrosine residues. There are a total of 8 tyrosine residues in the intracellular domain of PDGFRA and the signaling molecules that interact with these tyrosine residues have also been identified [14]. Functions of these downstream signaling molecules in the mediation of PDGFRA signaling are tissue context dependent, and PI3K-mediated PDGFRA signaling is the major intracellular cascade in the regulation of survival and proliferation in skeletal development via p53 [15].

In mouse, Pdgfra was broadly expressed in the primitive endoderm and mesoderm derivatives thorough embryogenesis, Pdgfra mRNA was detected in the visceral endoderm at E6.5, later after gastrulation, Pdgfra mRNA was detected in many mesenchyme derivatives, including the somites, limb bud and branchial arches [16, 17, 18]. Deletion of Pdgfra induced embryonic lethality at around E11, and multiple development defects in Pdgfra null embryos [12, 13, 19]. However, early death of Pdgfra null embryos precluded the functional investigation of Pdgfra in urorectal development [13]. Abnormal PDGF signaling has recently been shown to associate with defective external genitalia development in human [20].

To address the temporal requirement of Pdgfra in urorectal development, we conditionally deleted Pdgfra in Pdgfra-expressing tissues at different embryonic stages using a tamoxifen inducible Cre-loxP approach in mice, examined the urorectal development in Pdgfra conditional knockout embryos. We showed that conditional deletion of Pdgfra in Pdgfra-expressing tissues at E10-E11 caused cloaca septation defect, abnormal urethra tubularization in mice. Furthermore, our data also showed that Pdgfra was required for the survival of urorectal mesenchyme in normal development, deletion of Pdgfra caused cell death of the urorectal mesenchyme.

Methods and materials

Generation of ethylenethiourea induced rat models of anorectal malformations

Ethylenethiourea (ETU) solution was prepared by dissolving ETU powder in water to give a final concentration of 1% (W/V), and stored at 4 °C. Outbred Wister rats (250–300 g) of 10 to 12 weeks of age were mated, and appearance of vaginal plug in the female rat the morning after mating was timed as the gestational day 1. The pregnant rats were given a single dose of ETU at gestational day 11 by gavage feeding (12.5 ml/kg body weigh). ETU treated and un-treated litters were collected at E14.5. Urorectal regions of treated embryos ($n = 9$) with ARM phenotypes and un-treated control embryos ($n = 8$) were dissected for RNA isolation and processed for Microarray analysis using GeneChip® expression arrays Rat Expression Set 230 or for real-time PCR validation. Labelling, hybridization and signal detection were performed following standard protocols. Genes identified to be up or down-regulated in ETU treated ARM embryos were

confirmed by real-time PCR analysis on a separate biological replicates.

Mice and genotyping

The $Pdgfra^{fl/fl}$ [13] and $Pdgfra^{Cre/ERT}$ ($B6N;SJL$-$Tg(Pdgfr$-a-$cre/ERT)467Dbe/J$) [21] mouse strains were purchased from The Jackson Laboratory. The $Pdgfra^{fl/fl}$ mice were maintained in $C57BL/6JEi$, the $Pdgfra^{Cre/ERT}$ mice were maintained in $C57BL/6NJ$. All mice were supplied with food and water ad libitum, and kept under pathogen-free condition with a 12 h light/dark cycle. The morning the vaginal plug was observed was considered as embryonic day 0 (E0). All the animal experiment protocols were approved by the Committee on the Use of Live Animals in Teaching & Research, The University of Hong Kong (CULATR No.: 3123–13, 3368–14; 3566–15).

Genotyping

Genomic DNA was extracted from 2 mm tail clip using PBND extraction method. PCR genotyping of mice and copy number assay to distinguish $Pdgfra^{Cre/ERT}$; $Pdgfra^{fl/fl}$ ($Pdgfra$-cKO) and $Pdgfra^{Cre/ERT}$; $Pdgfra^{fl/+}$ were performed as described [22].

Tamoxifen induction

Tamoxifen stock (20 mg/ml of corn oil) was prepared by warming tamoxifen (Sigma) in corn oil and 0.1 mg per gram of body weight was administered by intragastric gavage to pregnant mice.

Histology examinations

Embryos were fixed in PFA/PBS (4% (w/v) paraformaldehyde (Sigma-Aldrich, Steinheim, Germany) in PBS (phosphate-buffered saline, pH 7.2; Sigma-Aldrich, Steinheim, Germany)) for 36 h at 4 °C, dehydrated in graded series of alcohol (Merck, Darmstadt, Germany), cleared in xylene (RCI Labscan Ltd, Bangkok, Thailand) before being embedded in paraffin (Leica Biosystems, Richmond, IL USA). Sections (8 μm in thickness) were prepared, mounted onto TESPA-coated microscope glass, and stained with hematoxylin and eosin following standard protocol. Photos were taken with the Olympus SZX7 microscope mounted with the Olympus DP71 High Resolution Color Digital Camera.

TUNEL assay

Apoptotic cells on sections were detected using In Situ Cell Death Detection Kit following manufacturer's protocol

(Roche Applied Science, Indianapolis, IN, USA). Images were taken with Nikon Eclipse 80i microscope (Melville, NY, USA) mounted with SPOT RT3 microscope digital camera (DIAGNOSTIC Instruments, Inc., Sterling Heights, MI, USA) under fluorescence illumination for the DAPI + ve nuclei and TUNEL + ve cells. Photos were compiled using Adobe Photoshop 7.

To quantitate the apoptosis of the mesenchyme surrounding the urethra and cloaca, photos of the TUNEL stained coronal sections of the urorectum of the control and $Pdgfra$-cKO embryos were taken, total number of cells of the peri-urethra and peri-cloaca mesenchyme were quantitated by counting DAPI + ve nuclei and apoptotic cells were quantitated by counting TUNEL + ve nuclei. Percentages of apoptotic cells of the respective regions of $Pdgfra$-cKO and control embryos were calculated by (TUNEL + ve nuclei/DAPI + ve nuclei) x100%. Eight embryos of each group were included for the analysis, six sections of each embryos of the urethra and cloaca region were examined for the quantitation of the apoptosis. Percentages of apoptosis were shown as mean ± S.D.

Statistical analysis

Student's t Test was performed to calculate the differences between groups, and p value less than 0.05 was regarded as statistically significant.

Western blotting

Urorectal tissues (0.5 g) of $Pdgfra$-cKO and control littermates were harvested and homogenized with 1 ml Lysis Buffer on ice for 30 s (For 1 ml Lysis Buffer, 100 μl 10xLysis Buffer (Bio-Rad), 10 μl of PI (Protease Inhibitor, Bio-Rad) and 1 μl of PMSF (0.1 M in isopropanol, Bio-Rad) were added). After homogenization, the lysates were centrifuged at 14,000 rpm for 30 min at 4 °C, and the supernatant was transferred to new tubes and stored at −80 °C.

Pooled extracted protein (20 μg) of 6 urorectum was resolved by electrophoresis on a standard 8% denaturing polyacrylamide gel, and then electro-transferred onto PVDF membranes using mini Trans-blot cell (Bio-Rad, Hercules, CA, USA). After transfer, the PVDF membrane was rinsed by TBS-T (pH 7.6), and then blocked with 5% non-fat milk in TBS-T for 2 h. After washing with TBS-T for 5 min twice, the membrane was incubated with corresponding primary antibody (Supplementary Table 1) at 4 °C overnight by gentle shaking. Followed by washing with TBS-T for 15 min thrice, the membrane was incubated in HRP-conjugated secondary antibody for 2 h by gentle shaking. The membrane was rinsed with TBS-T for 15 min thrice with gentle shaking to remove the unbound secondary

antibody. Signals were visualized by ECL assay (GE Healthcare Amersham ECL and Western Blotting Detection System) following manufacturer's protocol, and detected by SYNGENE GBox-F3-E. The molecular weight of the positive band was determined by comparing their molecular weight with proper protein ladder (Fermentas, Gern Burnie, MD, USA) on the membranes.

RT-PCR analysis and real-time PCR (qPCR) analysis

RNA was extracted from E12.5 urorectum using RNeasy® Mid Kit (Qiagen) according to the manufacturer's protocol. The extracted RNA was treated with gDNA Eraser to remove genomic DNA. Complementary DNA was synthesized using (PrimeScript™ RT reagent Kit with gDNA Eraser, Perfect Real Time, Cat. #RR047Q) following the manufacturer's protocol.

PCR was performed in 25 μl of reaction mixture containing PCR buffer (Roche); $MgCl_2$ (2.5 mM); dNTP (0.2 mM each); forward and reverse primers (0.1 nmole each); 3 μl DNA template and 2.5 units DNA polymerase (QIAGEN; HotStart Taq), with 1% Betanine. Amplification was performed with forward and reverse primers specific for *Pdgfra* and *18s RNA*. Primers: *Pdgfra*-forward, 5′-GGACTTACCCTGGAGAAGTGAGAA-3′; *Pdgfra*-reverse: 5′-ACACCAGTTTGATGGATGGGA-3′; *beta-actin*-forward: 5′-ACCCGCGAGCACAGCTTCTTT-3′; *beta-actin*-reverse: 5′-GGAGCCGTTGTCGACGACCA-3′. The initial denaturation was performed at 95 °C for 5 min, PCR reaction was performed with appropriate cycle numbers described as follows: 30 s denaturation at 95 °C, 60 s annealing at specific temperature, 60 s extension at 72 °C for each cycle. An additional extension step was carried out for 10 min at 72 °C. PCR products were analyzed by electrophoresis in a 1.5 % (w/v) agarose gel and stained by ethidium bromide which was visualized under UV illumination.

Real-time PCR analysis was performed on 7900HT Fast Real-Time PCR system using Fast SYBR Green Master Mix (Applied Biosystems, Foster City, USA), and were performed in triplicate on 6 biological replicates. Relative expression levels of *Pdgfra* in urorectal tissues were determined using *beta-actin* as internal reference and $2^{-\Delta\Delta Ct}$ method. The relative expression of *Pdgfra* between controls and mutants were calculated taking the relative expression level of *Pdgfra* in controls arbitrarily as one, and expressed as mean ± S.E.M..

Scanning electron microscopy

Urorectal regions of E14.5 and E18.5 *Pdgfra-cKO* and control littermates were dissected and fixed in 2.5% glutaraldehyde (Merck) in 0.1 M cacodylate buffer (Merck) for 24 h at 4 °C, washed in 0.1 M cacodylate buffer pH 7.4 before second fixation in 1% osmium tetroxide (aqueous) (Merck) pH 7.4 for 1 h at room temperature. After washings in 0.1 M cacodylate buffer pH 7.4, tissues were dehydrated in a series of graded ethanol until 100% (EM grade). Critical point drying of dehydrated tissues were performed on Bal-tec CPD 030 Critical Point Dryer (BAL-TEC AG—Balzers, Liechtenstein), and sputter coating of tissues were performed on Bal-tec SCD 005 Sputter Coater (BAL-TEC AG—Balzers, Liechtenstein) according to manufacturer's protocols. Samples were examined on Hitachi S-4800FEG scanning electron microscope (Tokyo, Japan).

Immuno-histochemistry

Paraffin sections (8 μm in thickness) were prepared and mounted onto TESPA-coated glass slides. Sections were dewaxed in xylene, hydrated in a graded series of alcohol and finally in distilled water. Endogenous peroxidase activity was quenched by incubation of section in methanol containing 3% H_2O_2 at room temperature for 30 min. After washing in water, antigen was retrieved by incubating in 10 mM sodium citrate buffer (pH 6.0) at 95 °C for 10 min. After blocking in PBS-T (PBS with 0.1% Triton) supplemented with 1% Bovine Serum Albumin (USB Corporation, Cleveland, OH USA) for 1 h at room temperature, sections were incubated with anti-PDGFRA antibody (Abcam ab124392; 1:100 dilution) in PBS-T supplemented with 1% Bovine Serum Albumin or Ki67 antibody (BD Pharmigen 556003; 1:100 dilution) in Mouse Ig Blocking Reagent (M.O.M.™ Immunodetection Kits, Vector Laboratories) for overnight at 4 °C. The sections were washed in PBS and secondary body incubation and signal development were performed using EnVision Detection Systems Peroxidase/DAB, Rabbit/Mouse system (Dako) or M.O.M.™ Immunodetection Kits (Vector Laboratories) according to manufacturer's protocol. After washing in water, sections were counterstained with Haematoxylin, washed in water, incubated in 2% (W/V) $NaHCO_3$ for 30 s before being washed in water. Sections were dehydrated in a graded series of alcohol, dewaxed in xylene and then mounted in DPX mountant (BDH). Images were taken with Nikon Eclipse E600 microscope mounted with Nikon Digital Camera DXM1200F.

Whole mount beta-galactosidase activity staining

Embryos were fixed in PFA/PBS for 1 h at 4 °C. X-gal/IPTG staining was performed at 37 °C for 18 h as describe previously [23]. Stained embryos were fixed in PFA/PBS at 4 °C for 18 h, dehydrated in graded series of alcohol, cleared in toluene (RCI Labscan Ltd, Bangkok, Thailand) before being embedded in paraffin. 10 μm thick sections

were prepared and mounted onto TESPA-coated microscope glasses. Sections were dewaxed in toluene, hydrated in graded series of alcohol before being completely hydrated in water, counter-stained with Nuclear Fast Red according to manufacturer's protocol (Vector Lab. Inc. Burlingham, CA), and mounted in Faramount Aqueous Mounting Medium (Dako).

In situ hybridization

For section ISH, embryos were fixed in 4% paraformaldehyde, embedded in paraffin wax and sectioned in 6 μm. ISH was performed following standard protocols.

Results

Ethylenethiourea induced urorectal developmental anomalies and down-regulation of Pdgfra in rat embryos

Ethylenethiourea (ETU) induces anorectal malformations (ARMs) in rat fetuses, providing an ideal animal model to study the pathogenesis of ARMs [24]. ETU-treated embryos displayed urorectal defects which are typified in human ARMs, including delayed genital tubercle outgrowth; incomplete cloaca septation and untubularized urethra [25]. We performed Affymetrix GeneChip (Rat Expression Set 230) analysis in normal and ETU-treated rat embryos with urorectal anomalies to identify genes/pathways implicated in urorectal development. GeneChip analysis followed by real-time PCR analysis in biological replicates identified *Pdgfra* down-regulation in ETU-treated embryos (Supplementary Figure 1). Immuno-histochemistry confirmed ETU induced down-regulation of Pdgfra, disrupting the spatial-temporal distribution of Pdgfra at the developing urorectum (Supplementary Figure 1).

Pdgfra was tempo-spatially expressed in the urorectal mesenchyme during genital tubercle outgrowth and cloaca septation

Immuno-histochemistry for Pdgfra was performed on E10.5–E14.5 mouse embryo sections to investigate the tempo-spatial expression of Pdgfra in the developing urorectum from the stage of genital tubercle outgrowth to the completion of cloaca septation. At E10.5, immunoreactivity for Pdgfra was localized at the mesenchyme surrounding the cloaca of the budding genital tubercle (Fig. 1). At E11.5–E12, Pdgfra expressions were detected at most of the genital tubercle, urorectal septum and the hindgut mesenchyme. At E12.5, the urorectal septum developed further, moved downward to the cloaca

membrane. The cloaca membrane was consisted of a signal layer of cell. The Pdgfra expression was detected in the mesenchyme of the entire genital tubercle. At E13.5, septation of cloaca nearly completed with the openings of separated urogenital sinus and hindgut connecting to the outside. Pdgfra was expressed in the urorectal septum mesenchyme, in the mesenchyme surrounding the cloaca membrane and the urogenital sinus (Fig. 1). At E14.5, septation completed with the urethral duct and anal opening formation, Pdgfra was further restricted to the mesenchyme adjacent to the urethra and the ureter, to the urorectal septum and at the urethral plate mesenchyme. Expression of Pdgfra in most of the developing urorectal mesenchyme from E10.5 to E14.5 suggested that Pdgfra may be crucial for the genital tubercle outgrowth and the cloaca septation.

Tamoxifen inducible Cre-mediated deletion of gene in *Pdgfra*-expressing tissues in mouse urorectum

Tamoxifen (Tm) administration at E9.5 induced X-gal expression to the mesenchyme of the budding genital tubercle of male and female *Pdgfra*^{Cre/ERT}; *R26R* embryos as early as 24 h after Tm administration (filled arrowheads; Supplementary Figure 2A). However, a single dose of Tm at E9.5 was insufficient to induce X-gal expression to all the *Pdgfra*-expressing urorectal mesenchyme cells at the later embryonic stages in *Pdgfra*^{Cre/ERT}; *R26R* embryos (compared Fig. 1 and Supplementary Figure 2).

To improve the efficacy of Cre-mediated recombination in the *Pdgfra*-expressing urorectal mesenchyme, we gave Tm to pregnant females for two consecutive days at E9.5 and E10.5, harvested embryos at E11.5 and E14.5 for examination (Fig. 2). Strong X-gal staining was observed in the peri-cloaca mesenchyme of E11.5 *Pdgfra*^{Cre/ERT}; *R26R* embryos (Fig. 2b). By E14.5, X-gal staining was detected at most of the urorectal mesenchyme including the apical genital mesenchyme, genital tubercle mesenchyme, urethral plate mesenchyme, urogenital fold mesenchyme, and the mesenchyme surrounding the urethra (Figs. 2d, e). No X-gal staining was detected in *R26R* embryos (Figs. 2a, c). Therefore, two consecutive Tm administrations at E9.5 and E10.5 was sufficient to induce Cre-mediated recombination to most of the *Pdgfra*-expressing urorectal mesenchyme cells at the later embryonic stages.

Conditional knockout of *Pdgfra* in *Pdgfra*-expressing urorectal tissues in embryos resulted in cloaca septation defects

To investigate the impact of the conditional knockout of *Pdgfra* in *Pdgfra*-expressing urorectal tissues on the urorectal development, we gave Tm to pregnant females at E9.5 for two consecutive days at E9.5 and E10.5, harvested
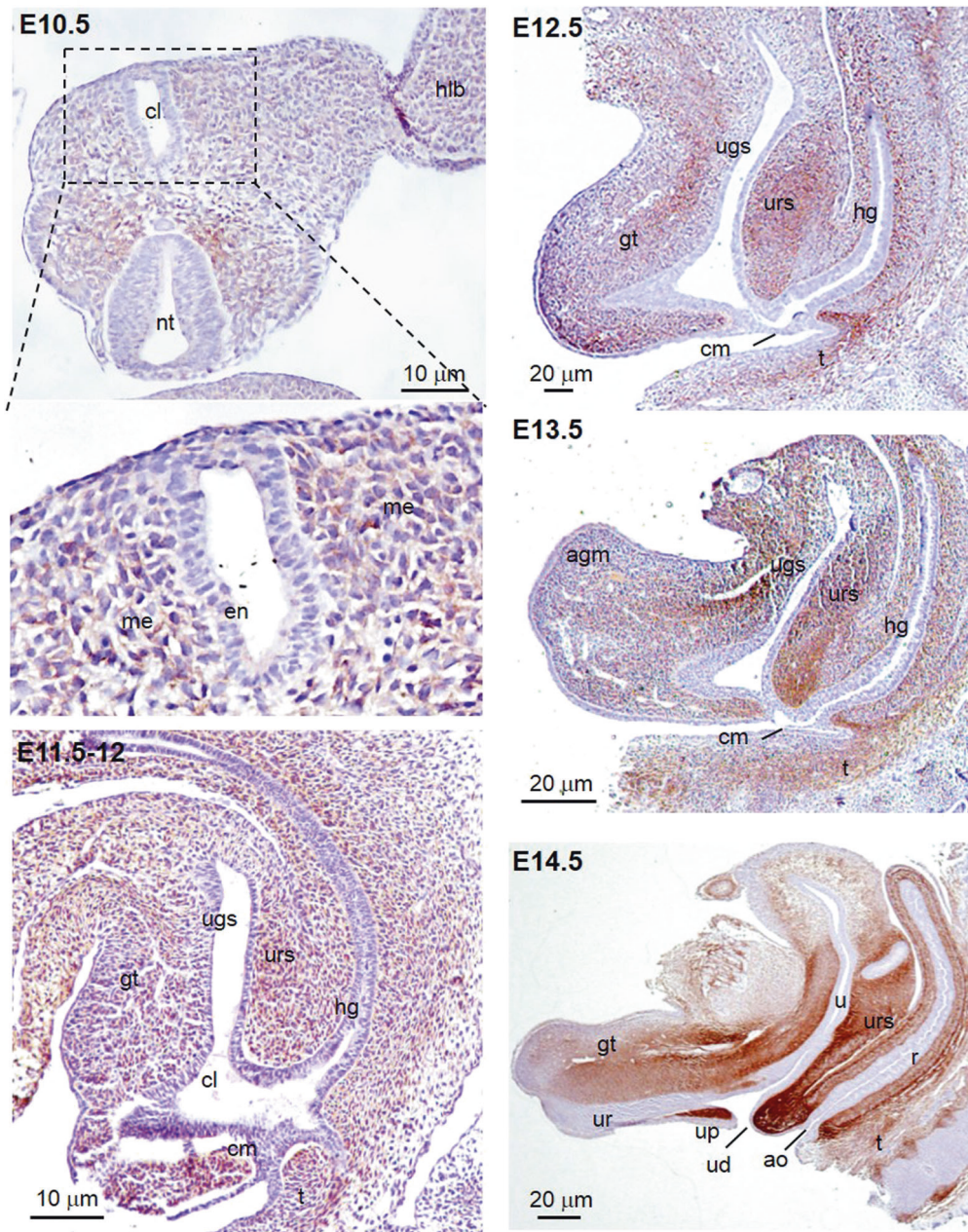
Fig. 1 Pdgfra was expressed in the peri-cloaca and genital tubercle mesenchyme of mouse embryos from E10.5 to E14.5. Immuno-histochemistry for Pdgfra was performed on transverse section of E10.5 and mid-sagittal sections of E11.5–E14.5 mouse embryos. Immuno-reactivity for Pdgfra (brown) was localized at the mesenchyme surrounding the cloaca of the budding genital tubercle at E10.5. From E11.5 to E13.5, Pdgfra expression was detected at the genital tubercle, urorectal septum and the hindgut mesenchyme. At E14.5, a more restricted expression of Pdgfra was localized at the mesenchyme adjacent to the urethra and the ureter, at the urorectal septum and at the urethral plate mesenchyme. *cl* cloaca, *hlb* hindlimb bud, *nt* neural tube *gt* genital tubercle, *ugs* urogenital sinus, *urs* urorectal septum, *hg* hindgut, *cm* cloaca membrane, *t* tail, *ur* urethra, *up* urethral plate, *ud* urethral duct, *ao* anal opening, *u* ureter, *r* rectum

embryos at E14.5 and E18.5 for examination (Fig. 3). Male and female E14.5 and E18.5 *Pdgfra* conditional (*Pdgfra-cKO*) embryos of the Tm treatment group were recovered in compliance with the expected Mendelian inheritance. Significant reduction of the expression of *Pdgfra* mRNA and Pdgfra protein in E14.5 *Pdgfra-cKO* urorectal tissues were shown by RT-PCR analysis, qPCR analysis and Western blot analysis (Figs. 4a-c). Absence of Pdgfra expression in the urorectal mesenchyme of E12.5 *Pdgfra-cKO* was confirmed by immuno-histochemistry (Fig. 4d).

At E14.5, the sizes of the genital tubercle of male and female *Pdgfra-cKO* embryos were comparable with that of control embryos as revealed by scanning electronic microscopy (SEM) study (Fig. 5). In the genital tubercle of both
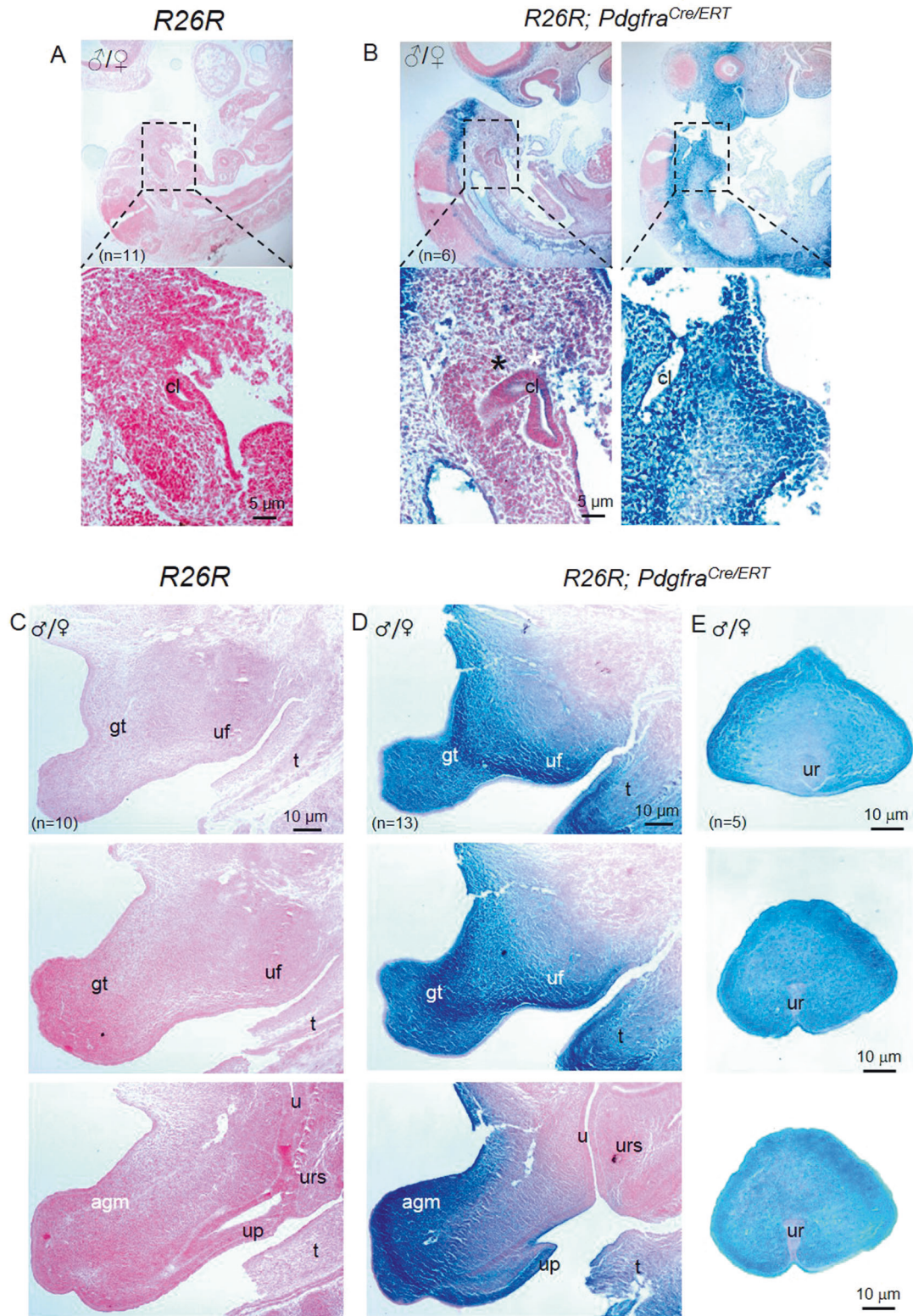
Fig. 2 *Pdgfra*[Cre/ERT] drives tamoxifen induced Cre recombination to the peri-cloaca and genital tubercle mesenchyme in mice. Tamoxifen was given to pregnant mice at E9.5 and E10.5, embryos were collected at E11.5 (**a**, **b**) or at E14.5 (**c**, **d**) for X-gal staining and sectioning. Strong X-gal staining was only observed in *R26R*; *Pdgfra*[Cre/ERT] embryos but not in *R26R* embryos. Region highlighted was shown underneath. *cl* cloaca, *gt* genital tubercle, *u* ureter, *urs* urorectal septum, *up* urethral plate, *uf* urogenital fold, *agm* apical genital mesenchyme, *t* tail. *n* = number of embryos analyzed
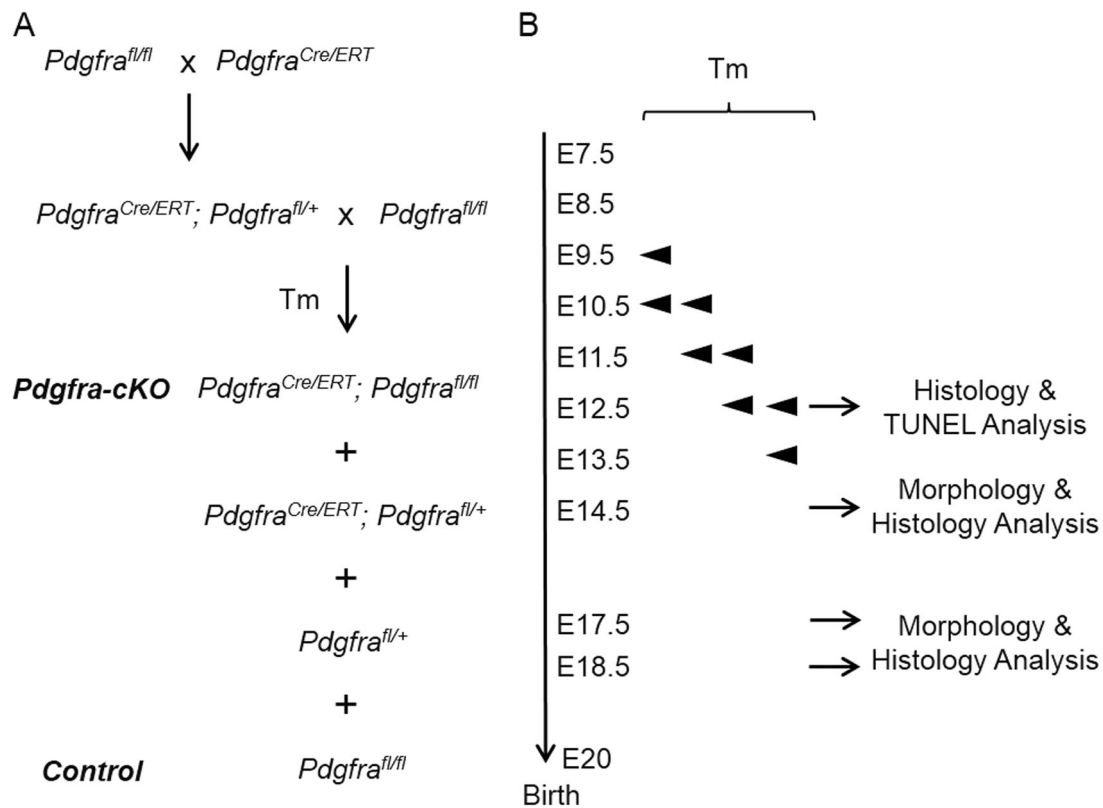
Fig. 3 Conditional deletion of *Pdgfra* in *Pdgfra*-expressing tissues in mouse embryos. **a** Crossing scheme of *Pdgfra^{Cre/ERT}* mice with *Pdgfra^{fl/fl}* to generate conditional knockout (*Pdgfra-cKO*, *Pdgfra^{Cre/}* *^{ERT}*; *Pdgfra^{fl/fl}*) and control (*Ctrl*, *Pdgfra^{fl/fl}*) embryos. **b** Tamoxifen (Tm) was given to pregnant females at various embryo days by intragastric gavage, and embryos were collected for analysis

male and female E14.5 *Pdgfra-cKO* embryos, there was an abnormal opening on the ventral side of the genital tubercle and the urogenital folds were missing. The prepuce and the labioscrotal folds developed normally in *Pdgfra-cKO* embryos.

Medial to lateral sagittal sections of E14.5 *Pdgfra-cKO* and control embryos were examined to investigate the process of cloaca septation in normal and *Pdgfra-cKO* embryos. In E14.5 normal embryos, the urorectal septum has elongated from the ventral body wall to the cloaca membrane. The proximal cloaca membrane regressed and the apical urotectal septum endoderm approximated to the cloaca membrane leading to the formation of the urethral duct and the anal opening, which signified the completion of cloaca septation (Fig. 5). In contrast, in both male and female *Pdgfra-cKO* embryos, the ventral elongation of the urorectal septum to the cloaca membrane was retarded and the apical urorectal septum endoderm did not approximate to the cloaca membrane, together with regression of the cloaca membrane and the urethral plate, a single opening was formed at the ventral side of the genital tubercle, the ureter and the rectum opened into this common opening. In addition, the urogenital fold were not developed normally in female and male *Pdgfra-cKO* embryos (Fig. 5).

At E18.5, the sizes of the genital tubercle of male and female *Pdgfra-cKO* embryos were comparable to that of control embryos (Fig. 5). From ventral view, there was an abnormal distal to proximal urethral opening along the ventral side of the genital tubercle in male and female *Pdgfra-cKO* embryos, in that prepuce and urethra were not developed normally and were not fused ventrally in *Pdgfra-cKO* embryos. Mid-sagittal sections of *Pdgfra-cKO* and control embryos revealed that the distance from the anal opening to the tail base was lengthened in *Pdgfra-cKO* embryos of both genders, which indicated that anal openings were anteriorly displaced in *Pdgfra-cKO* embryos.

We also gave tamoxifen to pregnant mice from the crossing at E10.5/11.5; E11.5/12/5 and E12.5/13.5, collected embryos at E14.5 and/or E17.5 for histology and morphology analysis. Urorectal defects could only be detected in the *Pdgfra-cKO* embryos of the E10.5/11.5 Tm group, but in general, with lower incidence and milder severity of the abnormalities. Only one E14.5 mutant *Pdgfra-cKO* embryo of E10.5/11/5 Tm group showed severe genital tubercle detects as that of 9.5/10.5 Tm group, but all the other *Pdgfra-cKO* embryos only displayed milder genital tubercle defects which included slightly enlarged urethral opening at E14.5 and incomplete ventral midline
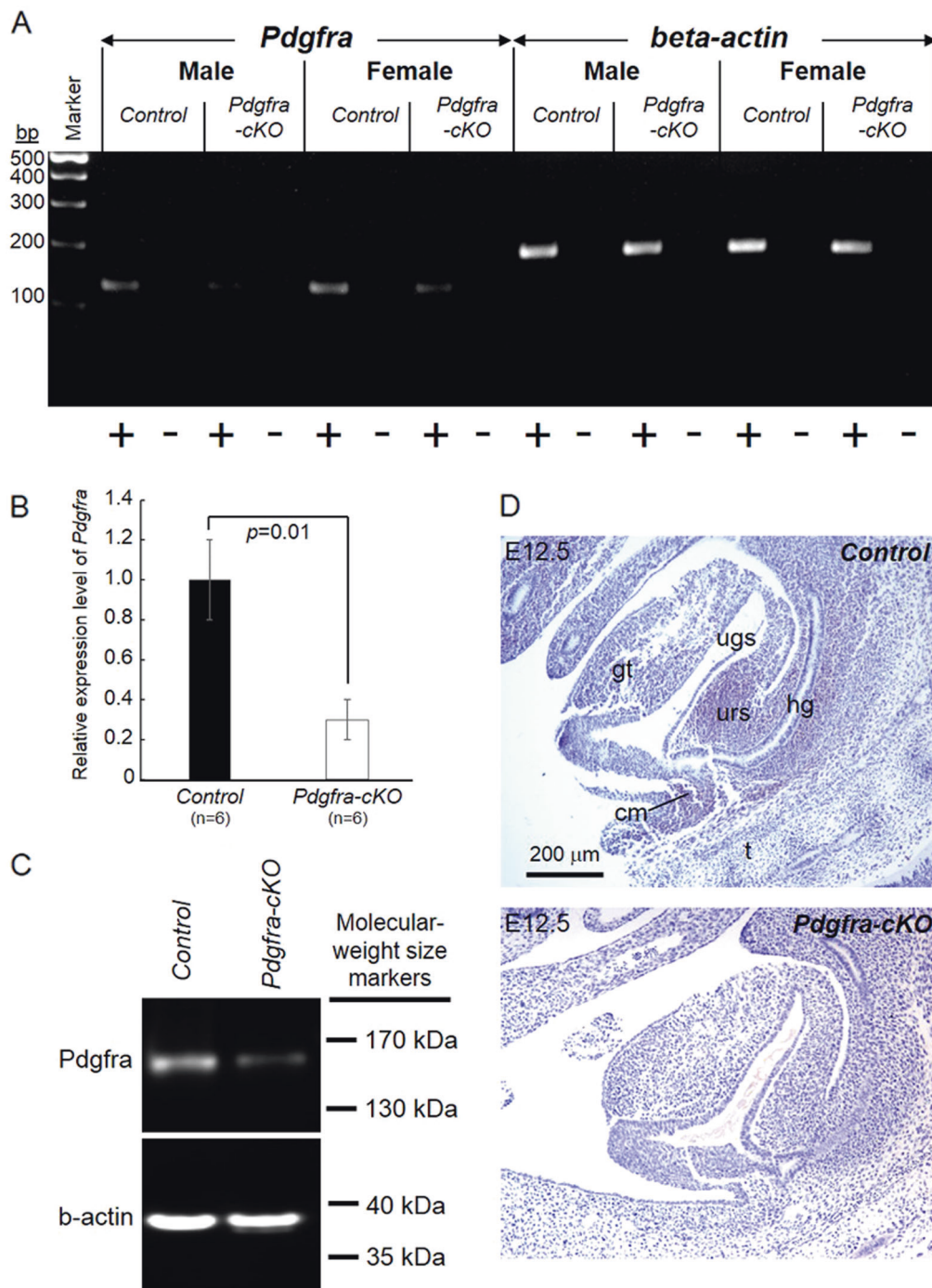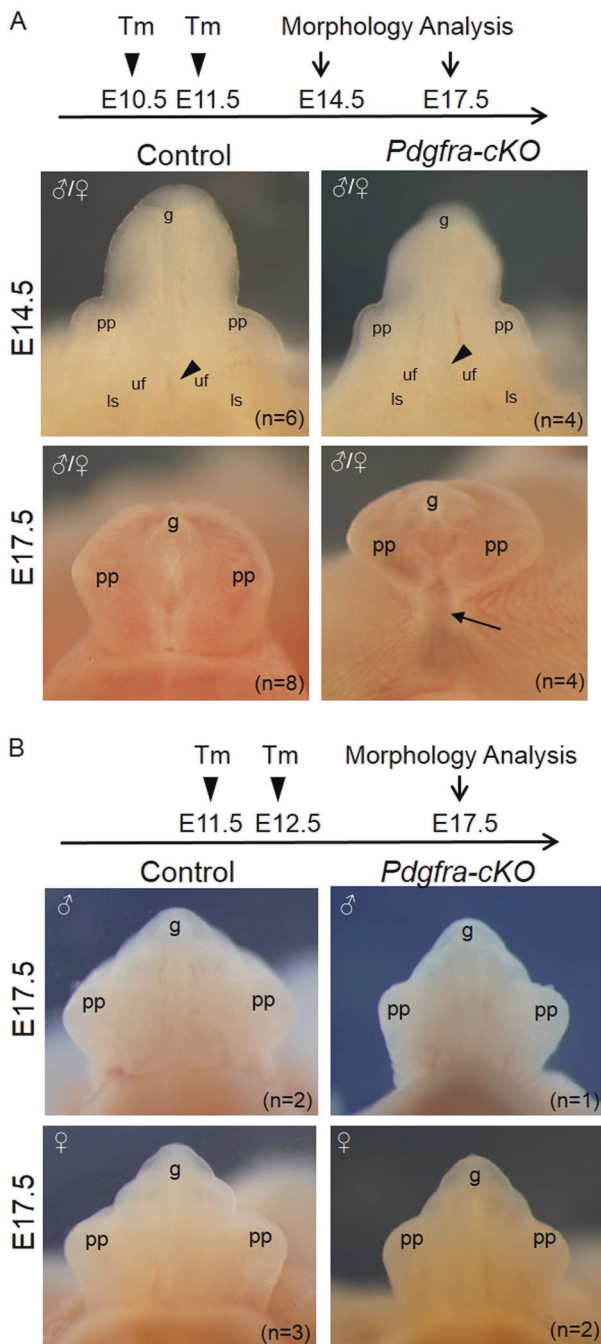
Fig. 4 Conditional deletion of *Pdgfra* in mouse embryos. Tamoxifen was given to pregnant mice at E9.5 and E10.5, E14.5 embryos were collected to isolate total RNAs of the urorectum for RT-PCR analysis (**a**) and qPCR analysis (**b**). Expression of *beta-actin RNA* was used as internal control. "+" means with RT; "−" means without RT (negative control). Relative expression levels of *Pdgfra* (mean ± S.E.M.) in control and mutant urorectum were shown and the relative expression level of *Pdgfra* in controls were taken arbitrarily as one. Western blot analysis was performed on E14.5 urorectum to detect the expression of Pdgfra and beta-actin (b-actin) was used as loading controls (**c**). E12.5 embryos were collected for immuno-histochemistry (**d**). Pdgfra expression (brown) was detected in the urorectal mesenchyme of E12.5 control embryos. In contrast, no Pdgfra expression was detected in the urorectal mesenchyme of E12.5 *Pdgfra-cKO*. *gt* genital tubercle, *ugs* urogenital sinus, *urs* urorectal septum, *hg* hindgut, *cm* cloaca membrane. *n* = number of embryos analyzed
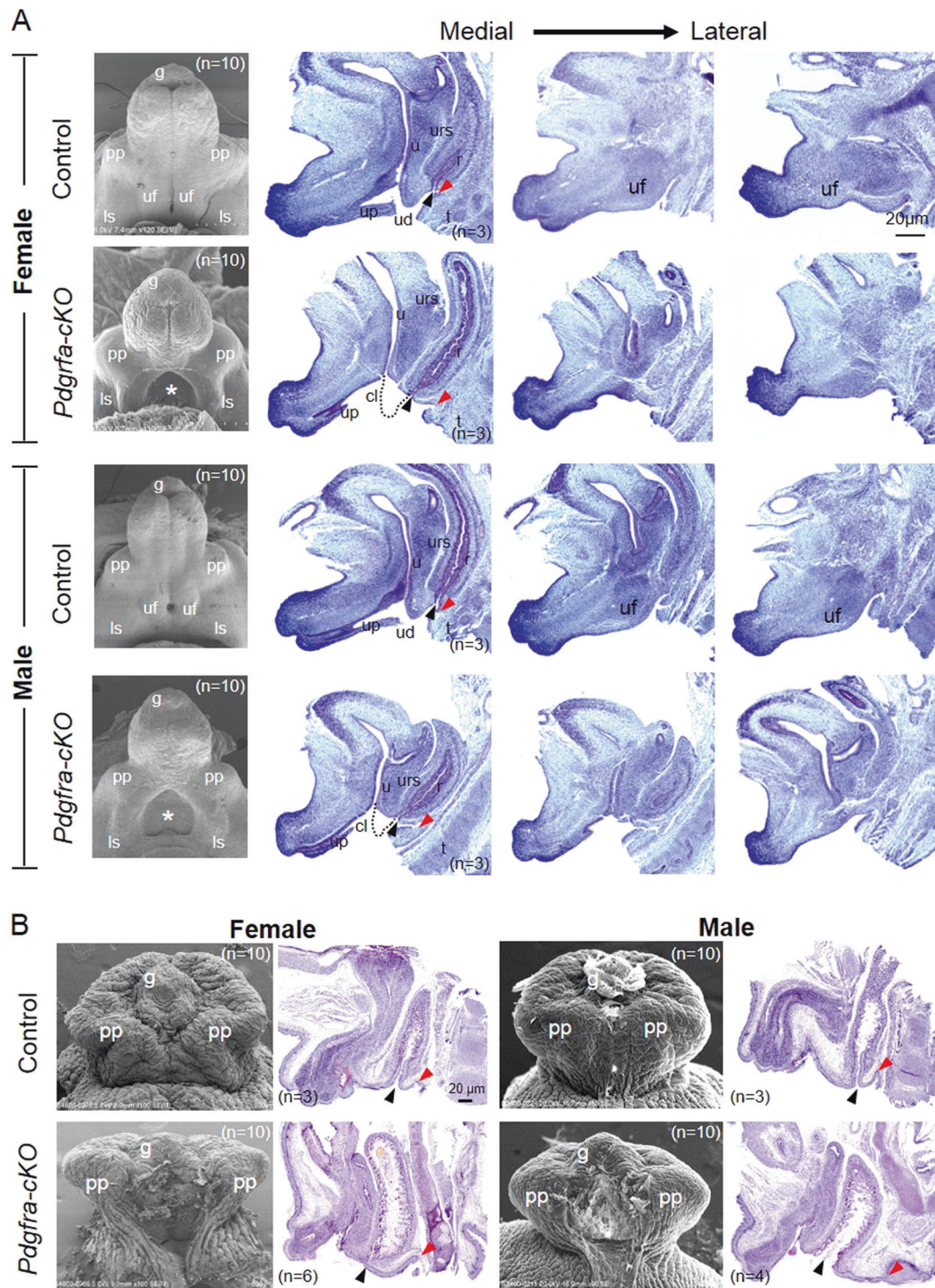
Fig. 5 Conditional deletion of *Pdgfra* in the mesenchyme of the developing external genitalia causes defective external genitalia development. Tamoxifen was given to pregnant mice at E9.5 and E10.5, embryos were collected at E14.5 (**a**) and E18.5 (**b**) for scanning electron microscopy and histology analysis. Medial to lateral sagittal sections of E14.5 control and *Pdgfra* conditional knockout (*Pdgfra-cKOs*) embryos revealed that the urorectal septum (urs) and the urogenital fold (uf) were not developed normally in female and male *Pdgfra-cKOs*. The urs was shorter and not reaching the level of the cloaca membrane in *Pdgfra-cKOs* (dotted lines indicated the expected normal locations of the urs). Prepuce and urethra were not developed normally in E18.5 male and female *Pdgfra-cKOs*. Anal openings were anteriorly displaced in male and female *Pdgfra-cKOs*. Red arrowhead indicates the location of the tail base. Black arrowhead indicates the anal opening. *pp* prepuce, *uf* urogenital fold, *ls* labioscrotal fold, *urs* urorectal septum, *r* rectum, *u* urethra, *cl* cloaca, *up* urethral plate, *ud* urethral duct, *t* tail, *g* glans. *n* = number of embryos analyzed

Fig. 6 Conditional deletion of *Pdgfra* in the mesenchyme of the developing external genitalia at later embryonic stages resulted in milder defective external genitalia development. Tamoxifen was given to pregnant mice at E10.5 and E11.5 (**a**) or E11.5 and E12.5 (**b**), embryos were collected at E14.5 and/or E17.5 for morphology analysis. Black arrowhead indicates the location of the urethral opening. Black arrow indicates the proximal untubularized urethra. *pp* prepuce, *uf* urogenital fold, *ls* labioscrotal fold, *g* glans. *n* = number of embryos analyzed

fusion of prepuce and proximal untubularized urethra (Fig. 6a). No genital tubercle defects could be detected in all

the *Pdgfra-cKO* embryo of E11.5/12.5 and E12.5/13.5 Tm groups (Fig. 6b and data not shown).

Urorectal anomalies of *Pdgfra-cKO* embryos of different Tm groups were summarized as shown in Table 1.

Deletion of *Pdgfra* induced apoptosis of the urorectal mesenchyme

To test if deletion of *Pdgfra* induced apoptosis of the *Pdgfra*-expressing urorectal tissues in embryos, *Pdgfra-cKO* and control E12.5 embryos were examined by TUNEL assay. Apoptotic cells were abundantly localized at the mesenchyme surrounding the cloaca and the urethra; at the urorectal septum, apical genital mesenchyme and the urethral plate of male and female *Pdgfra-cKO* embryos (Figs. 7a, b). In contrast, apoptotic cells were only localized at the tip of the urethra and at the proximal cloaca membrane in normal E12.5 embryos. Percentages of the apoptotic cells in the peri-urethra and the peri-cloaca mesenchyme were significantly elevated in *Pdgfra-cKO* embryos as compared to that of control littermates (Fig. 7c).

Pdgfra regulates survival and proliferation in skeletal development via suppression of p53 [15]. Deletion of *Pdgfra* induced a marked production of p53 protein and the phosphorylation of p53 at the serine 46 position in mutants (Fig. 8). In line with the p53 induction of the transcription of its target gene *Ndrg1* (N-myc downregulated gene 1) and Ndrg1 is necessary for p53-dependent apoptosis [26], Ndrg1 protein level was markedly increased in mutant urorectum. Elevated Nrdg1 induced a cleavage of inactive Caspase-3 to active form of Caspase 3 (C-Caspase-3), causing cell apoptosis of the urorectal mesenchyme of male and female *Pdgfra-cKO* embryos.

Immuno-histochemistry for Ki-67 (proliferative cell marker) on sections of *Pdgfra-cKO* and control E12.5 embryos indicated that the proliferation of the urorectal mesenchyme of male and female *Pdgfra-cKO* embryos were largely unaffected by the deletion of *Pdgfra* (Supplementary Figure 3).

Discussion

This study shows for the first time that *Pdgfra* is required for the cloaca septation and urethra tubularization of the urorectal development, and deletion of *Pdgfra* in embryos causes cloaca septation defect, leading to abnormal urethra tubularization in mice. Furthermore, our data also shows that *Pdgfra* is required for the survival of urorectal mesenchyme in normal development, deletion of *Pdgfra* causes death of the urorectal mesenchyme and defective cloaca septation.

Table 1 Genital tubercle (GT) defects of *Pdgfra-cKO* embryos of different Tm groups

Tm	Collection	Embryos (*n*)	*Pdgfra-cKO* (*n*)	GT defects (*n*)
E9.5/10.5	E14.5	146 (M:64; F:82)	37 (25%) (M:17; F:20)	+(37)
	E18.5	143 (M:78; F:65)	39 (27%) (M:12; F:27)	+(39)
E10.5/11.5	E14.5	18 (M:8; F:10)	5 (27%) (M:2; F:3)	+(1); ±(4)
	E17.5	24 (M:13; F:11)	7 (29%) (M:3; F:4)	±(7)
E11.5/12/5	E17.5	8 (M:3; F:5)	3 (37%) (M:1; F:2)	−(4)
E12.5/13.5	E17.5	8 (M:4; F:4)	3 (37%) (M:1; F:2)	−(4)

Time of collection, number of total embryos and mutant embryos, genders, % of *Pdgfra-cKO* embryos, GT defects and number of mutants (in parenthesis) showing different GT defects of different Tm treatment groups were indicated. "+": severe GT defects include the urorectal septum retardation, urogenital fold dysplasia, no ventral midline fusion of prepuce and untubularized urethra. "±": mild GT defect includes slightly enlarged urethral opening, incomplete ventral midline fusion of prepuce, and proximal untubularized urethra. "−": no GT defect

Tm tamoxifen, *M* male, *F* female

The correct time and level of *Pdgfra* expression during embryonic development are critical for the proper development of the urorectal mesenchyme and its derivatives. The *Pdgfra*-expressing mesenchyme at E10.5 (genital tubercle outgrowth phase) derived into the peri-cloacal mesenchyme, the urs mesenchyme, the apical genital mesenchyme and the lateral mesenchyme of the urethra at E14.5. When *Pdgfra* was deleted at around E10.5 (E9.5 + E10.5 Tm group), excessive apoptosis was detected at the mesenchyme of all these regions of E12.5 *Pdgfra-cKO* mouse embryos, which resulted in urorectal defects at E14.5. Urorectal defects with lower incidence and milder severity could only be detected in the *Pdgfra-cKO* embryos when *Pdgfra* was deleted at around E11.5 (E10.5 + E11.5 Tm group). Furthermore, *Pdgfra-cKO* embryos did not develop any urorectal anomaly if *Pdgfra* was deleted at around E12.5 (E11.5 + E12.5 Tm group) and at E13.5 (E12.5 + E13.5 Tm group). Taken all these indicated that tempo-spatial expression of *Pdgfra* in the developing urorectal mesenchyme between E10.5 and E11.5 was critical for cloaca septation and subsequent urorectal development in mice.

The excessive cell death of the urorectum disturbed the ventral elongation of the urs and the cloaca septation, as well as urs proximal-distal movement along the ventral edge of the genital tubercle. In addition, the excessive cell death of the apical genital mesenchyme and the peri-urethra mesenchyme also caused defective growth and folding of the genital tubercle mesenchyme. As the consequences of the apoptosis and the defective growth of the urs, the apical genital and the peri-urethra mesenchyme, the urethral folds fail to form and fuse along the ventral midline of the genital tubercle, leading to incomplete urethra tubularization and a big "hole" at the genital tubercle root at E14.5 and at the perineum at E18.5.

We also discovered that deletion of Pdgfra induced a production of p53, an apoptotic factor, and phosphorylation of p53 at the position of Serine 46 (p-p56(Ser46)) in uroerctum. It has been shown that p53 induced the transcription of *Ndrg1* (N-myc downregulated gene 1) and Ndrg1 was necessary for p53-dependent apoptosis via activation of Caspase 3 [26]. In line with p53 induction of Ndrg1, we observed elevated Ndrg1 protein level and production of active Caspase 3 (C-Caspase-3) and cell death in *Pdgfra-cKO* urorectum.

We have crossed *Pdgfra*^{fl/+};*Pdgfra*^{Cre/ERT} mice with *Pdgfra*^{fl/fl} mice and administered Tm at E7.5 and E8.5, only few *Pdgfra-cKO* embryos could be collected at E14.5 and no *Pdgfra-cKO* embryos could survive up to E17.5. It demonstrated that conditional deletion of *Pdgfra* at early embryonic stage prior to E9.5 resulted in early embryonic lethality, which was consistent with the phenomenon reported in *Pdgfra*−/− mutant embryos [13].

In mice, genital tubercle outgrowth starts at around E10. In both the E12.5 and the E14.5 *Pdgfra-cKO* mutants of the E7.5 Tm and E8.5 Tm groups, genital tubercle outgrowth appeared largely unaffected but the mutant genital tubercles were smaller (data not shown). In addition, genital tubercle outgrowth of mutant embryos of E9.5 Tm and E9.5 + E10.5 Tm groups also proceeded normally, but the mutant genital tubercles were smaller. Taken all these together may suggest that deletion of *Pdgfra* prior to genital tubercle outgrowth was insufficient to cause genital tubercle outgrowth defect. However, one has to be cautious in interpreting the data because the efficiency of the Cre-mediated deletion of *Pdgfra* has to be determined to examine if the lack of genital tubercle outgrowth defect is the consequence of insufficient deletion of *Pdgfra* in these mutants. *Pdgfra* displays sexual dimorphic expression pattern in gonad, regulates testis organization and Leydig cell differentiation of early testis development [27]. However, it is not known if early testis developmental defect in *Pdgfra*−/− mice affects the subsequent urethra tubularization of male external genitalia.

Pathways and transcription factors such as SHH, BMP, FGF, WNT, Eph/ephrin, and HOX family have been implicated in the urorectal development. These signaling

Fig. 7 Elevated cell death of the urorectal mesenchyme of Pdgfra-conditional knockout embryos. Transverse (**a**) and mid-sagittal (**b**) sections of E12.5 mutant and control embryos were analyzed using TUNEL analysis. **c** Percentages of apoptotic cells in the peri-urethra and peri-cloaca mesenchyme of wild-type (filled bar) and *Pdgfra-cKO* embryos (un-filled bars) were shown. Apoptotic cells (red) were abundantly localized at the mesenchyme surrounding the cloaca and the urethra (**a**); at the urorectal septum, apical genital mesenchyme and the urethral plate of the mutant embryos. In contrast, apoptotic cells were localized only at the tip of the urethra (future urethra orifice) and at the cloaca membrane. Regions highlighted with dotted line were magnified and shown on the right. *ur* urethra, *cl* cloaca, *agm* apical genital mesenchyme, *up* urethral plate, *ut* urethral tip, *cm* cloaca membrane *urs* urorectal septum. *n* = number of embryos analyzed
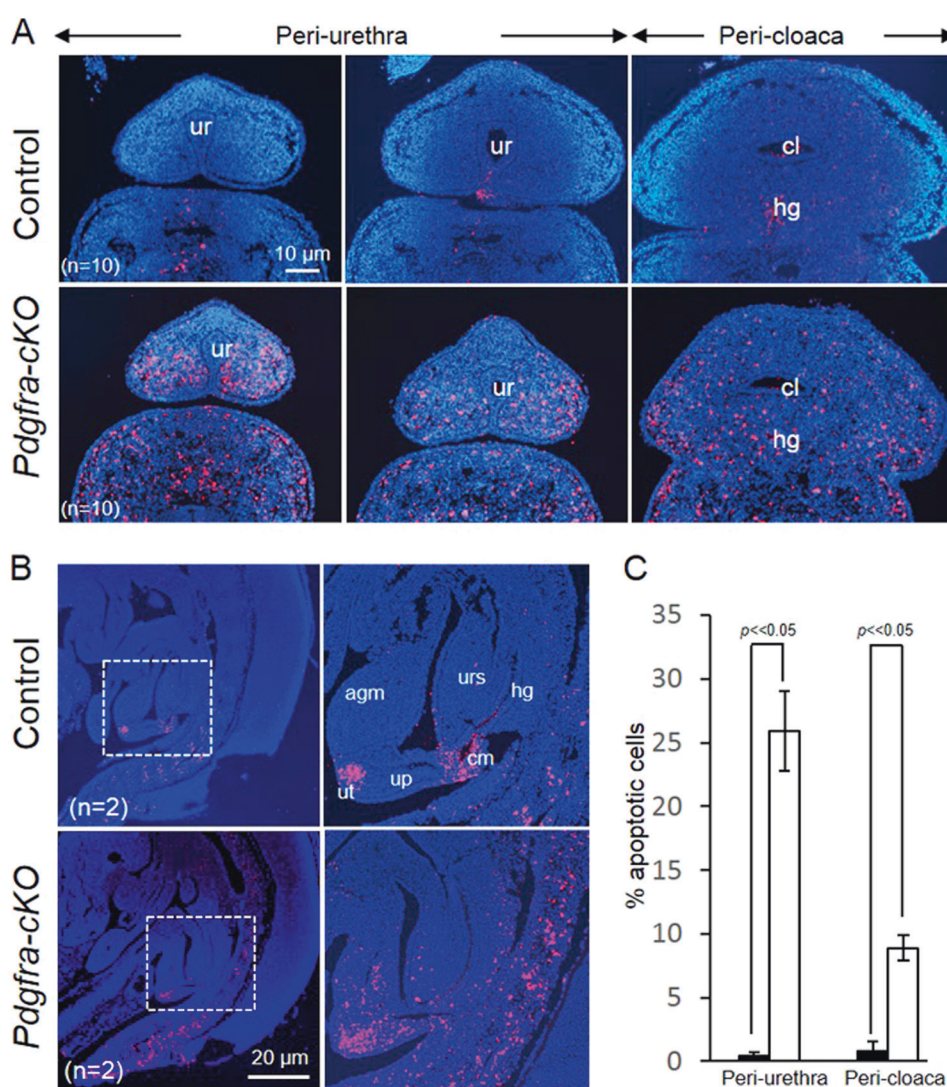
pathways or factors coordinated with each other to regulate the urorectal development and participate in the regulation of cell apoptosis [25]. *Bmp4* expression at the apical genital mesenchyme and at the urethral plate mesenchyme was slightly down-regulated in the *Pdgfra-cKO* mutant genital tubercles of E9.5 + E10.5 Tm group (Supplementary Figure 4). Bmp4 have been demonstrated to mediate cell apoptosis in several tissues [28, 29, 30, 31]. *Pdgfra* has also been suggested to be a target of Gli factors, linking Hh and PDGF signaling [32]. The interactions between PDGFRA signaling and other signaling pathways in the regulation of urorectal development worth further investigation in future.

In summary, Pdgfra is required for the process of cloaca septation. Elevated apoptosis was detected in the peri-cloacal, the peri-urethra mesenchyme and the urs mesenchyme of *Pdgfra-cKO* mutants, associated with an induction of p53 and activation of caspase-3 in *Pdgfra-cKO* embryos. Dysregulated Pdgfra signaling induced urorectal defects resembling human congenital diseases include the anorectal malformations and hypospadias. Therefore, perturbation of PDGFRA signaling may contribute to anorectal malformations and hypospadias in human.

In conclusion, we demonstrated a temporal and spatial requirement for Pdgfra mediated signaling in the urorectal development, and its dysregulation could cause urethra tubularization defects and hypospadias-like phenotypes in mice.

Compliance with ethical standards
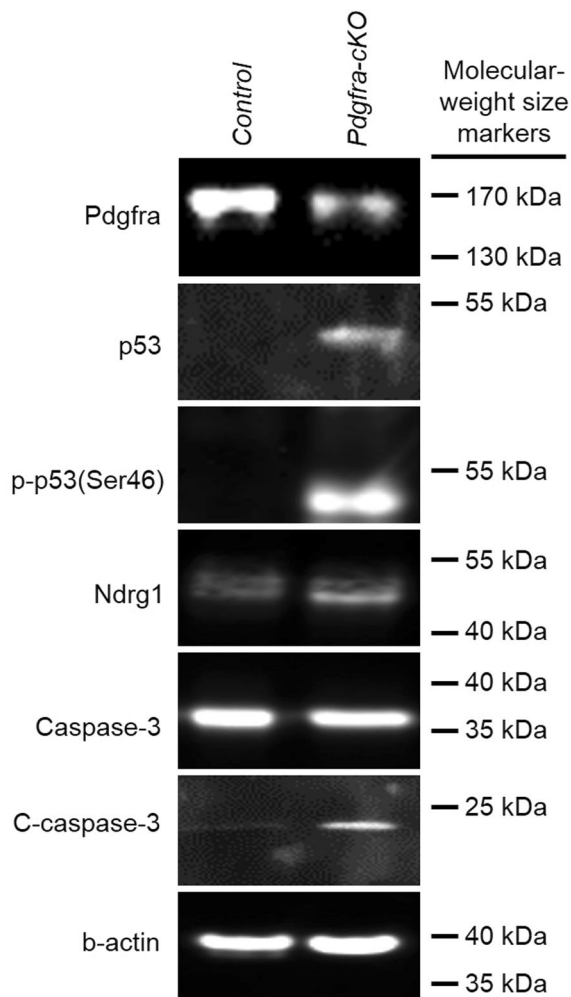
Fig. 8 Deletion of *Pdgfra* induced phosphorylation of p53 and activation of Caspase 3 in the genital tubercle. Tamoxifen was given to pregnant mice at E9.5 and E10.5, embryos were collected at E12.5 to isolate protein of the urorectum. Proteins of 6 *Pdgfra-cKO* and control urorectum were pooled and separated by polyacrylamide gel electrophoresis. Expressions of Pdgfra, Caspase 3, activated Caspase 3 (C-Caspase 3), p53, phosphorylated p53 (p-p53(Ser46)), Ndrg1 and beta-actin (b-actin) were analyzed by western blotting

References

1. Perriton CL, Powles N, Chiang C, Maconochie MK, Cohn MJ. Sonic hedgehog signaling from the urethral epithelium controls external genital development. Dev Biol. 2002;247:26–46.
2. Cohn MJ. Development of the external genitalia: conserved and divergent mechanisms of appendage patterning. Dev Dyn. 2011;240:1108–15.
3. Springer A, van den Heijkant M, Baumann S. Worldwide prevalence of hypospadias. J Pediatr Urol. 2016;12:152 e151–157.
4. Kohler N, Lipton A. Platelets as a source of fibroblast growth-promoting activity. Exp Cell Res. 1974;87:297–301.
5. Ross R, Glomset J, Kariya B, Harker L. A platelet-dependent serum factor that stimulates the proliferation of arterial smooth muscle cells in vitro. Proc Natl Acad Sci USA. 1974;71:1207–10.
6. Westermark B, Wasteson A. A platelet factor stimulating human normal glial cells. Exp Cell Res. 1976;98:170–4.
7. Bergsten E, Uutela M, Li X, Pietras K, Ostman A, Heldin CH, et al. PDGF-D is a specific, protease-activated ligand for the PDGF beta-receptor. Nat Cell Biol. 2001;3:512–6.
8. LaRochelle WJ, Jeffers M, McDonald WF, Chillakuru RA, Giese NA, Lokker NA, et al. PDGF-D, a new protease-activated growth factor. Nat Cell Biol. 2001;3:517–21.
9. Li X, Ponten A, Aase K, Karlsson L, Abramsson A, Uutela M, et al. PDGF-C is a new protease-activated ligand for the PDGF alpha-receptor. Nat Cell Biol. 2000;2:302–9.
10. Heidaran MA, Pierce JH, Yu JC, Lombardi D, Artrip JE, Fleming TP, et al. Role of alpha beta receptor heterodimer formation in beta platelet-derived growth factor (PDGF) receptor activation by PDGF-AB. J Biol Chem. 1991;266:20232–7.
11. Matsui T, Heidaran M, Miki T, Popescu N, La Rochelle W, Kraus M, et al. Isolation of a novel receptor cDNA establishes the existence of two PDGF receptor genes. Science. 1989;243:800–4.
12. Hoch RV, Soriano P. Roles of PDGF in animal development. Development. 2003;130:4769–84.
13. Soriano P. The PDGF alpha receptor is required for neural crest cell development and for normal patterning of the somites. Development. 1997;124:2691–2700.
14. Heldin CH, Westermark B. Mechanism of action and in vivo role of platelet-derived growth factor. Physiol Rev. 1999;79:1283–316.
15. Fantauzzo KA, Soriano P. PI3K-mediated PDGFRalpha signaling regulates survival and proliferation in skeletal development through p53-dependent intracellular pathways. Genes Dev. 2014;28:1005–17.
16. Orr-Urtreger A, Bedford MT, Do MS, Eisenbach L, Lonai P. Developmental expression of the alpha receptor for platelet-derived growth factor, which is deleted in the embryonic lethal Patch mutation. Development. 1992;115:289–303.
17. Orr-Urtreger A, Lonai P. Platelet-derived growth factor-A and its receptor are expressed in separate, but adjacent cell layers of the mouse embryo. Development. 1992;115:1045–58.
18. Schatteman GC, Morrison-Graham K, van Koppen A, Weston JA, Bowen-Pope DF. Regulation and role of PDGF receptor alpha-subunit expression during embryogenesis. Development. 1992;115:123–31.
19. Tallquist MD, Soriano P. Cell autonomous requirement for PDGFRalpha in populations of cranial and cardiac neural crest cells. Development. 2003;130:507–18.
20. Geller F, Feenstra B, Carstensen L, Pers TH, van Rooij IA, Korberg IB, et al. Genome-wide association analyses identify variants in developmental genes associated with hypospadias. Nat Genet. 2014;46:957–63.
21. Kang SH, Fukaya M, Yang JK, Rothstein JD, Bergles DE. NG2 + CNS glial progenitors remain committed to the oligodendrocyte lineage in postnatal life and following neurodegeneration. Neuron. 2010;68:668–81.
22. Qian C, Wong CWY, Wu Z, He Q, Xia H, Tam PKH, et al. Stage specific requirement of platelet-derived growth factor receptor-alpha in embryonic development. PLoS One. 2017;12:e0184473.
23. Sanes JR, Rubenstein JL, Nicolas JF. Use of a recombinant retrovirus to study post-implantation cell lineage in mouse embryos. EMBO J. 1986;5:3133–42.
24. Qi BQ, Beasley SW, Frizelle FA. Clarification of the processes that lead to anorectal malformations in the ETU-induced rat model of imperforate anus. J Pediatr Surg. 2002;37:1305–12.
25. Ng RC, Matsumaru D, Ho AS, Garcia-Barcelo MM, Yuan ZW, Smith D, et al. Dysregulation of Wnt inhibitory factor 1 (Wif1) expression resulted in aberrant Wnt-beta-catenin signaling and cell death of the cloaca endoderm, and anorectal malformations. Cell Death Differ. 2014;21:978–89.
26. Stein S, Thomas EK, Herzog B, Westfall MD, Rocheleau JV, Jackson RS 2nd, et al. NDRG1 is necessary for p53-dependent apoptosis. J Biol Chem. 2004;279:48930–40.

27. Brennan J, Tilmann C, Capel B. Pdgfr-alpha mediates testis cord organization and fetal Leydig cell development in the XY gonad. Genes Dev. 2003;17:800–10.

28. Gambaro K, Aberdam E, Virolle T, Aberdam D, Rouleau M. BMP-4 induces a Smad-dependent apoptotic cell death of mouse embryonic stem cell-derived neural precursors. Cell Death Differ. 2006;13:1075–87.

29. Graham A, Francis-West P, Brickell P, Lumsden A. The signalling molecule BMP4 mediates apoptosis in the rhombencephalic neural crest. Nature. 1994;372:684–6.

30. Jernvall J, Aberg T, Kettunen P, Keranen S, Thesleff I. The life history of an embryonic signaling center: BMP-4 induces p21 and is associated with apoptosis in the mouse tooth enamel knot. Development. 1998;125:161–9.

31. Trousse F, Esteve P, Bovolenta P. Bmp4 mediates apoptotic cell death in the developing chick eye. J Neurosci. 2001;21:1292–301.

32. Lin C, Chen MH, Yao E, Song H, Gacayan R, Hui CC, et al. Differential regulation of Gli proteins by Sufu in the lung affects PDGF signaling and myofibroblast development. Dev Biol. 2014;392:324–33.